Comparison of solitary and collective foraging strategies of *Caenorhabditis elegans* in patchy food distributions

Siyu Serena Ding[1,2*], Leah S. Muhle[3,4*], André E. X. Brown[1,2], Linus J. Schumacher[3,5], Robert G. Endres[3]

[1]Institute of Clinical Sciences, Imperial College London, London, United Kingdom
[2]MRC London Institute of Medical Sciences, London, United Kingdom
[3]Department of Life Sciences, Imperial College London, London, United Kingdom
[4]Eberhard-Karls-Universität, Tübingen, Germany
[5]Present address: MRC Centre for Regenerative Medicine, University of Edinburgh, Edinburgh, United Kingdom

[*]These authors contributed equally.
Correspondence to: r.endres@imperial.ac.uk or linus.schumacher@ed.ac.uk

Abstract

The benefits of social behaviour in insects and vertebrates are well-documented in terms of mating success and predator avoidance. Social foraging has also been shown to benefit organisms in environments where food is patchily distributed, but whether this is true in the case where organisms do not rely on long-range communications to coordinate their social behaviour has been understudied. To address this question, we use the tractable laboratory model organism *Caenorhabditis elegans*, where a social strain (*npr-1* mutant) and a solitary strain (N2) are available for direct comparison of foraging strategies. We first develop an on-lattice minimal model for comparing social and solitary feeding strategies, finding that social agents benefit from feeding faster and more efficiently simply due to group formation. To compare these simulation results with real experimental data, we modify our minimal model to incorporate the specific feeding behaviours of the *npr-1* and N2 strains. Surprisingly, the resultant strain-specific model predicts that the solitary strain performs better than the social one in all food distribution environments that we tested, which we confirm with lab experiments. Additional computational experiments identify the N2 strain's higher feeding rate to be the key factor underlying its advantage over *npr-1* worms. Our work highlights the difficulties in addressing questions of optimal behaviour, and the valuable role of modelling as a guiding principle.

Keywords: *C. elegans*, collective behaviour, social feeding, foraging strategy, on-lattice simulation, fitness

Introduction

Collective behaviour is displayed in many animals like social insects, fish shoals, flocking birds, and mammals (1, 2). Collective behaviour may have evolved when benefits outweigh the costs, and the process is thought to be adaptive (i.e., increase an individual's fitness (3)). Possible benefits of collective behaviour may include a decreased risk of attack of an individual by a predator (4), faster and more reliable decision-making (5, 6) , and an increased probability of finding a mating partner (7). The costs of collective behaviour include competition for resources (8), investment in complex communication systems (9), and the opportunity cost of waiting for information (10) within the group.

Less well-understood is the effect of collective behaviour on foraging, although recent models and field experiments suggest that this collective search for food may improve food detection as well as food uptake (11-14). For instance, computational models showed that foraging in groups can provide an advantage for finding heterogeneously distributed food, albeit using long-range interactions (15). While long-range interactions may apply to animals with good visual or acoustic (3, 16) processing, this type of interaction may be less relevant for smaller mesoscopic animals with limited sensory modalities, including nematodes, whose collective foraging we know little about. Moreover, direct comparison between model predictions and experimental data is often limited by uncontrolled natural environments that the animals live in (17). The 1 mm-long roundworm *C. elegans* is not only small and transparent to enable easy imaging (18), but is also highly tractable on both the genetic (19-21) and the neural circuitry (22) level. Therefore we use *C. elegans* with its experimentally controllable environment to compare collective and solitary foraging strategies using both modelling and experimental approaches.

C. elegans worms feed on bacteria that proliferate in rotten fruits and stems (23). The food resource in the worms' natural environment fluctuates and is patchily distributed in space and time (24). Intriguingly, while *C. elegans* strains isolated from the wild exhibit varying degrees of collective feeding when grown in the lab (25), the laboratory reference strain N2 feeds individually. This striking difference led us to hypothesise that the contrasting foraging strategies may confer advantages in the strains' respective resource environments. That is to say, collective foraging may be beneficial for wild strains in their natural environments where food distribution is likely patchy, whereas solitary foraging may be better suited for the laboratory environment where food is omnipresent and virtually unlimited.

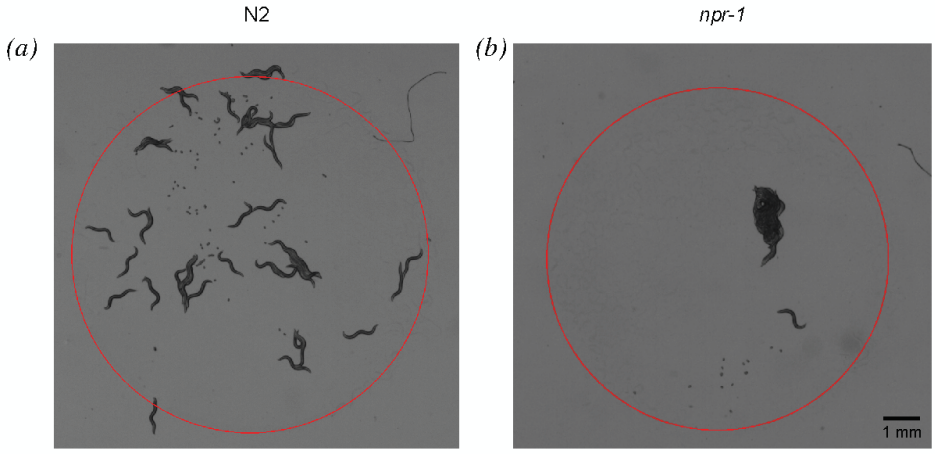

Figure 1: Snapshots of *C. elegans* on *E. coli* bacterial lawns from brightfield microscopy. *(a)* Solitary N2 worms on a bacterial lawn. *(b)* Hyper-social *npr-1(ad609)* worms on a bacterial lawn. Red circles indicate the food boundary.

To test this hypothesis, we experimentally model solitary versus social behaviour with N2 (Figure 1a) and *npr-1* (Figure 1b) worms, respectively. The latter are N2 worms with a loss-of-function mutation *(ad609)* in the neuropeptide receptor gene *npr-1*, and are hyper-social with pronounced group formation on food (25, 26). Thus N2 and *npr-1* worms represent opposite extremes of the collective phenotype and provide a useful system to compare social versus solitary foraging strategies in a genetic background that is identical except for the single *npr-1* gene. Apart from regulating foraging behaviour, the *npr-1* gene influences the

responses to O_2 levels and pheromones, as well as the susceptibility to pathogens, among other effects (27-29). Past work by us and others have examined the behavioural mechanisms of aggregate formation for these two strains (26) as well as the fitness consequences of their aggregation phenotypes (30); nevertheless, how their contrasting foraging strategies perform in diverse resource distribution environments remains unknown.

To examine whether collective foraging is more effective than solitary foraging in heterogeneously distributed food environments, we developed a lattice-based foraging model for movement and feeding based on local worm-worm interactions only (where the agents can only interact with other agents on directly adjacent lattice sites). First, we used a minimal model in which the only difference between social and solitary agents is their tendency to form groups on food. Simulation results from this model support the hypothesis that collective foraging can be beneficial in patchy food distribution environments, as social agents are both faster and more efficient at depleting food than solitary ones. These results motivated us to create a more realistic model that incorporates additional strain-specific behavioural parameters, in order to facilitate direct comparison with the experimental data. The more realistic model predicts that N2 is faster and more efficient at depleting food than *npr-1* for all tested food distribution conditions, which we confirmed in experiments. We conclude that the solitary N2 strain outperforms the social *npr-1* strain not necessarily via its foraging strategy. The difference could arise from N2 modifying other behaviours such as increasing its feeding rate or from aspects of the experiment not captured in the model.

Results

Collective foraging is beneficial in patchy food-distribution environments in the minimal model

The minimal model aims to determine whether collective foraging is more effective than solitary foraging in terms food intake. To achieve this, social and solitary agents are simulated to differ only in their ability to form groups on food. This allows us to examine the effect of foraging in groups alone, without any other complications such as different movement speeds between the agent types.

The minimal model is designed based on two experimental observations from literature and brightfield recordings of solitary N2 worms and social *npr-1* worms (Figure 1 and Supplementary Movies S1 and S2). Firstly, worms move faster off food than on food, presumably to find new food (31). To implement this, both solitary and social agents, with identical speeds, move to lattice sites in the *remote neighbourhood* in the absence of food and to lattice sites in the *direct neighbourhood* in the presence of food (Figure 2a). In our model, agents perceive food on the lattice site they are located on and on the lattice sites in their direct neighbourhood. Secondly, worms pump their pharynx and ingest bacteria while moving (32), which we simulate by letting both types of agents consume one food unit per time step if they are on food.

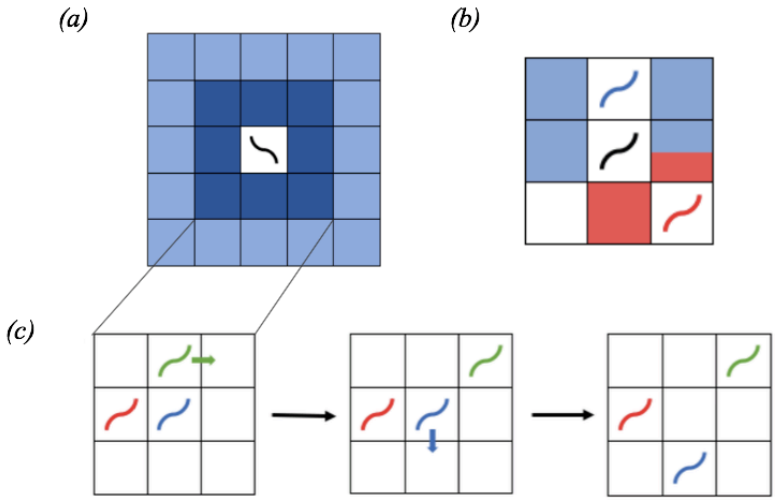

Figure 2: Schematics of neighbourhoods and computation of targeted steps. *(a)* Direct (dark blue) and remote (light blue) neighbourhoods of an agent (black worm) on a square lattice. *(b)* Possible motion updates of the black social agent performing a targeted step. Red squares show the direct neighbourhood shared by the red and the black agents, and blue squares show the direct neighbourhood shared by the blue and the black agents. Therefore, while performing a targeted step, the black agent is only allowed to move to the coloured squares to perform a targeted step to the direct neighbourhood of an adjacent agent. *(c)* Consecutive execution of targeted steps in a group of three agents. The order in which motion updates are computed is chosen randomly for every time step. The green agent performs the first targeted step and moves to a square adjacent to the blue agent. Subsequently, the blue agent executes a targeted step and moves to a square next to the red agent which isolates the green agent from the group. This shows that a targeted step may also separate agents from their group.

As a simplifying assumption, the movement of agents is modelled through random steps, unless an agent has neighbours in the presence of food. In the latter case, social agents try to join a group by switching from random steps to targeted steps towards nearby neighbours (Figure 2b,c) (15). By contrast, solitary agents always perform random steps (see flow chart in Figure S1a). Hence, the minimal model simulations are constructed exclusively for examining the influence of neighbour affinity on foraging (see Material and Methods for more details of the minimal model). We chose to ignore long-range chemotaxis by food or pheromone signalling as our previous work has suggested these are not important for the collective phenotypes of the two strains (26). We implement food distributions with different degrees of food clustering controlled by a parameter γ in a manner similar to (15), so that one food unit is placed a distance $d \geq 1$ away from an existing one with the probability $P(d) = d^{-\gamma}$ (see Materials and Methods). This parameterisation allows us to continuously vary

between a uniformly random ($\gamma = 0$) food distribution and distributions with increasing patchiness as γ is increased (Figure 3a).

In natural environments, *C. elegans* coexists with other nematodes competing for the same food resources, so fast and efficient food depletion may enable a species to outperform its competitors (23, 33). Thus we measured both time to 90% food depletion and foraging efficiency in our model simulations. In environments with uniform randomly distributed ($\gamma = 0$) or slightly patchy food ($\gamma \leq 1$), social agents need longer to deplete food than solitary ones (Supplementary Movies S3-4). When food is strongly patchy ($\gamma > 1$), social agents deplete food faster than solitary ones (Supplementary Movies S5-6). The crossover between the two foraging strategies can be found at approximately $\gamma \approx 1.5$ (Figure 3b). Overall, these results confirm our initial hypothesis, indicating that a solitary foraging strategy is beneficial in environments with uniformly distributed food whereas collective foraging prevails in environments with patchy food. Interestingly, restricting food perception to the agent's current lattice site diminishes the advantage of solitary agents in environments with uniformly random distributed or slightly patchy food ($\gamma \leq 1$) (Figure S2a).

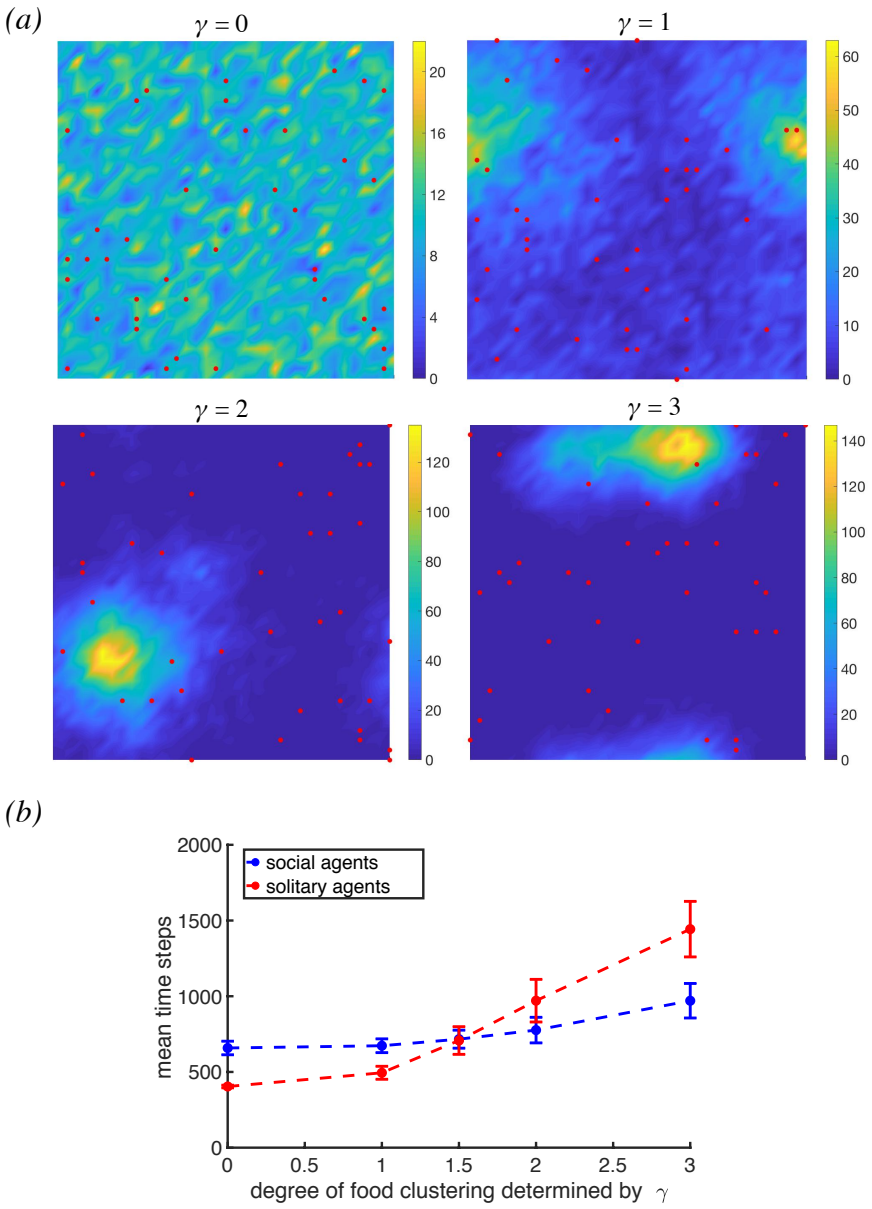

Figure 3: Food distributions used in minimal model simulations and time steps social and solitary agents need to deplete food. *(a)* Food distributions for different γ values. Red dots show the agents (distributed uniformly random in all cases), and the colour bars show the number of food units per lattice site. *(b)* Mean number of time steps taken by social and solitary agents to deplete 90% of the distributed food depending on the degree of food clustering, showing a crossover with social agents eating faster than solitary agents in patchy food environment (γ>1.5) and vice versa. Error bars show 1 SD.

The benefit of the collective foraging strategy remains when success is measured in terms of foraging efficiency (Figure S3a,b), which is computed for individual agents by dividing the total number of food units it consumes by the total number of steps it takes; similar benefit-cost trade-offs had been considered by others in previous works (34, 35). In environments with uniformly random or slightly patchy food ($\gamma \leq 1$), solitary agents forage with a higher

median efficiency than social ones, while the opposite is true in environments with patchy food distributions ($\gamma > 1$). However, the efficiencies of both social and solitary agents decrease as patchiness increases. At the individual level, food is distributed more evenly among solitary agents than among social ones in environments with uniformly random distributed food (Figure S3c,d). With restricted food perception, this effect disappears (Figure S2d,e), and the individual efficiencies of social and solitary agents resemble each other for $\gamma \leq 1$ (Figure S2b,c). These findings underline that collective foraging may be advantageous in environments with patchy food distribution due to the higher efficiency and thus lower energy expenditure.

Solitary foraging of N2 agents is more successful in all food distribution environments in strain-specific simulations

As the social *npr-1* and solitary N2 *C. elegans* strains vary in a number of behavioural parameters, next we incorporate these strain-specific differences into the minimal model in order to create a more realistic version of the model. We implement two main behavioural differences reported in literature: Firstly, the speeds of *npr-1* and N2 worms differ depending on food availability. Both strains move at roughly the same speed in the absence of food, but N2 worms slow down to roughly half this speed when on food, whereas *npr-1* worms only slow down significantly upon joining a group of worms on food (25). Secondly, *npr-1* and N2 worms exhibit different feeding rates, as calculated by us previously (36). These literature parameters are listed in Table 1 and adapted for our strain-specific simulations (model parameters are listed in Table 2). We also considered food-leaving probabilities, but food-leaving is extremely rare on the thin food lawns that we use for our experiments compared to what others have reported under different experimental conditions (37, 38). Food-leaving probability in our experiments are near zero (0.013±0.013 (mean ± standard deviation) events per worm per hour for *npr-1* and 0.025±0.025 events per worm per hour for N2, see

Supplementary Methods for details), which is consistent with our previous report that worms are mostly on food under the same experimental conditions (26), so we do not use different food-leaving rates in our simulations. Nevertheless, our strain-specific model is constructed so that different food-leaving rates can easily be incorporated to test additional parameter combinations (see Supplementary Methods and Supplementary Figure 1b for details).

Table 1: Literature values for *npr-1* and N2 behavioural parameters.

	reference	***npr-1***	**N2**
speed in the presence of food	(25)	183 µm/s	109 µm/s
speed in the absence of food	(25)	225 µm/s	232 µm/s
feeding rate	(36)	0.576 unit	1 unit

Table 2: List of parameters used in modelling simulations.

	minimal model		**strain-specific model**	
	social agents	**solitary agents**	***npr-1* agents**	**N2 agents**
Step length in the presence of food	to direct neighbourhood	to direct neighbourhood	**in a group**: to direct neighbourhood **alone**: to remote neighbourhood	to direct neighbourhood
Step length in the absence of food	to remote neighbourhood	to remote neighbourhood	to remote neighbourhood	to remote neighbourhood
Feeding rate	1 food unit/time step	1 food unit/time step	0.2304 food unit/time step	0.4 food unit/time step
Food-leaving probability	Not used	Not used	0	0

In this more realistic, strain-specific model, agents perceive food only at the lattice site that they occupy. As in the minimal model, social *npr-1* agents can join groups on food by performing targeted steps, whereas N2 agents can only perform random steps (see flow chart in Figure S1b). To compare simulation outcomes with experimental results, we chose food distributions that can be experimentally reproduced: food is distributed in one-, two-, or four-spot configurations whilst keeping the total amount of food constant (Figure 4a). Note that a food "spot" is conventionally referred as a food "patch", but here we use the term "spot" instead of "patch" for both strain-specific simulations and the corresponding experiments. This is to avoid confusion with the term "patchiness" (as opposed to uniformity), which in

this context would refer to the presence of *multiple* spots (as opposed to a single spot). Each "spot" itself has a uniform distribution of food.

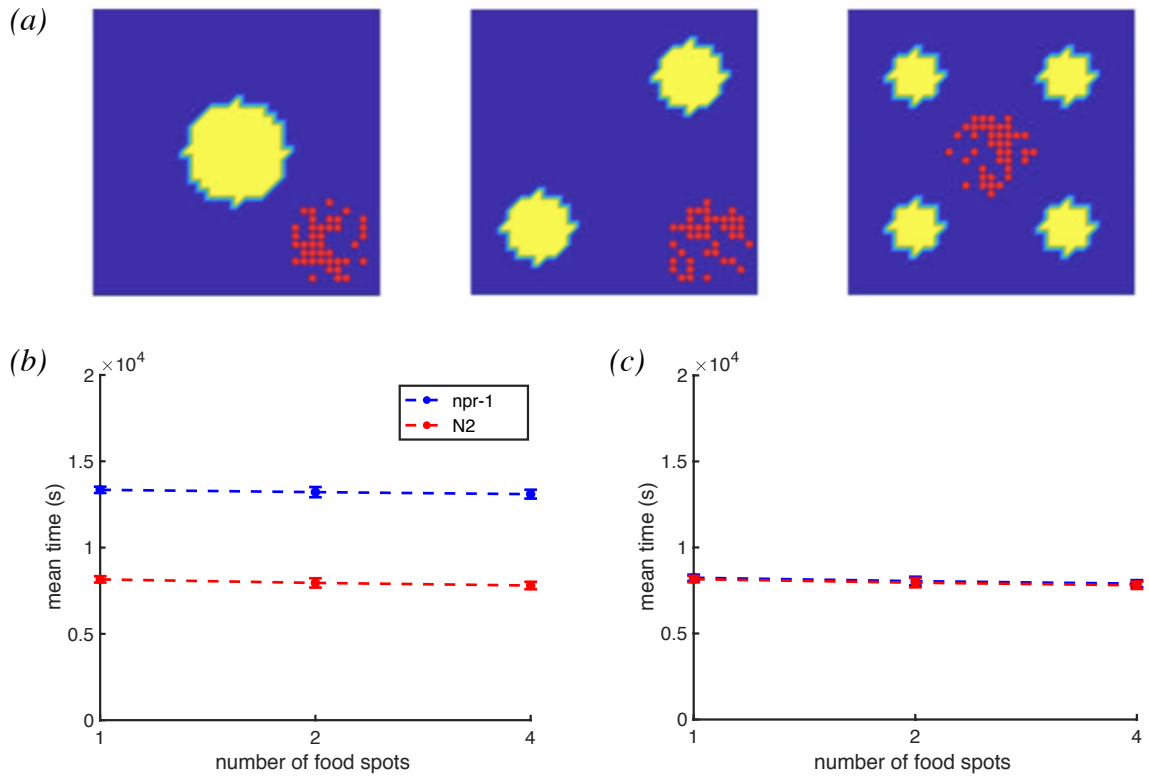

Figure 4: Food distributions used in strain-specific simulations and time steps *npr-1* and N2 agents need to deplete food. *(a)* Food distributions with one, two or four food spots. Red dots show agent configurations at the start of the simulations, with dark blue indicating no food and yellow indicating food. *(b)* Mean time for *npr-1* and N2 agents to deplete 90% of the distributed food units, shown for different numbers of food spots. Error bars show 1 SD. *(c)* Same as b), but with *npr-1* agent feeding rate set to the same value as N2. Simulation time is converted from time steps to real time in b) and c): as there is maximally a single agent per lattice site the lattice spacing is equal to the worm size (~ 1 mm). By noting that worm speed on food is approximately 100-200 µm/s and that it takes an agent one time step to cross the 1 mm lattice site, the timescale should be roughly $\Delta t \approx$5-10 s. Eventually Δt = 10 s is chosen to approximate the order of magnitude to broadly match the experimental data in Figure 5.

To assess the foraging success in this strain-specific model, we first calculated the time needed to deplete 90% of the distributed food for both *npr-1* and N2 agents. Social *npr-1* agents need longer than N2 to consume the same amount of food independent of the number of food spots (Figure 4b, Supplementary Movies S7-9). Furthermore, time to food depletion barely varies amongst different food spot number configurations for both *npr-1* and N2. Overall, now the solitary foraging strategy of N2 agents wins out in all tested food

distribution environments, which contrasts with the findings of the minimal model simulations. We also analysed the foraging efficiency of *npr-1* and N2. These results show that N2 agents forage with a substantially higher efficiency than *npr-1* in all tested conditions, even though the range of the individual efficiencies of N2 agents is larger compared to *npr-1* agents (Figure S4a,c). Apart from this, N2 agents have a marginally higher food intake in environments with one or two food spots than *npr-1* agents (Figure S4b,d; Figure S5a,b), indicating that individual N2 agents forage more successfully than *npr-1* individuals. However, fewer *npr-1* than N2 agents have an extremely low food intake in all environments (Figure S5a-c). This may suggest that the overall population survival of *npr-1* worms could be better than N2 when food is scarce, as fewer individual *npr-1* worms face starvation despite the lower overall foraging efficiency.

Experimental findings confirm predictions from the strain-specific model

To test the predictions of the strain-specific model, we conducted experiments with *npr-1(ad609)* mutants and N2 worms. For both worm strains, 40 age-matched young adults were imaged on low peptone NGM agar plates containing one, two, or four spots of *E. coli* OP50 bacteria (Figure 5a). The total amount of bacteria remains the same across different experiments regardless of the spot number (i.e., 20 µL for one spot, 10 µL per spot for two spots and 5 µL per spot for four spots; see Materials and Methods for further experimental details). Low peptone (0.13% w/v) in the media minimises bacterial growth during the experiment.

We measured the time the worms need to deplete the bacteria lawns. The end point of the assay is estimated from the detectable increase in worm speed once food becomes completely depleted (Figures S6). This can most clearly be seen in Supplementary Movies S1 and S2, where the texture of the background changes upon depletion from smooth to coarse, and the

dramatic speed-up of the worms can be visually detected. Figure 5b shows the mean time *npr-1* and N2 animals need to deplete different numbers of bacteria spots in the experiment. The N2 strain depletes bacteria faster than the *npr-1* strain independent of the number of bacteria spots. Thus, the experimental results confirm the prediction of the strain-specific model.

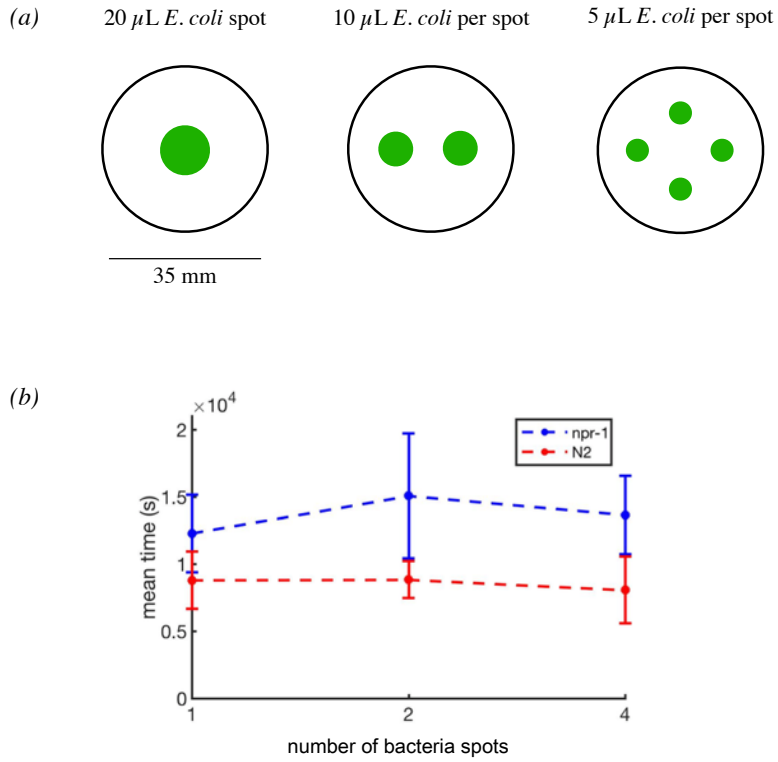

Figure 5: Food distribution used in experiments and time *npr-1* and N2 worms need to deplete bacteria in the experiments. *(a)* Schematics of *E. coli* spots (green) on imaging plates used in the experiments. *(b)* Mean time for 40 *npr-1* or N2 worms to deplete one, two, or four bacterial food spots in the experiments. Data is available for 3-4 independent replicates for each condition. Error bars show 1 SD.

Feeding rate is the key factor for N2's foraging advantage

To gain further insights into which aspect of the model determines the differences in performance between the two foraging strategies, the strain-specific simulations were repeated, but with equal feeding rates for *npr-1* and N2 agents (using the N2 value from Table 2). As a result, the difference between the strains in foraging time is completely abolished (Figure 4c). Furthermore, the distributions of individual efficiencies (Figure S4c,e) as well as of ingested food units (Figure S4d,f) for *npr-1* and N2 agents now resemble each other after

setting the feeding rates equal. These results suggest that the higher feeding rate of N2 is the main reason for its foraging advantage. The fact that there is no difference in foraging efficiency between the two strategies once the feeding rates have been made equal, is consistent with the patchy environment being roughly equivalent to a food distribution with $\gamma = 1.5$ where we also observed no difference in efficiency in the minimal model.

Discussion

We hypothesised that collective foraging in groups confers an advantage when foraging in environments with heterogeneously distributed food. To test this hypothesis we implemented lattice-based simulations, which are more computationally efficient than agent-based models (26) or spatial Gillespie simulations (39), and have a long history in ecological modelling (34). Unlike previous lattice-based simulations (15), we only allowed for short-range interactions in order to exclude the role of visual cues and long-range chemotaxis. Our approach is also different from other works which investigate optimal foraging in patchy environments based on the marginal value theorem (34, 35). Our minimal model confirms our hypothesis that foraging in groups can be beneficial in environments with patchy food distributions, as social agents deplete food faster and more efficiently than solitary ones. The simple presence of a worm may convey social information to other worms, such as indicating that food quality is sufficiently high (5, 17, 40). This type of swarm intelligence may be particularly valuable in the absence of sophisticated communication systems or long-range interactions.

In contrast to the minimal model, our more realistic strain-specific simulations show that the solitary N2 agents performs better than the social *npr-1* agents in environments with patchy food distributions (i.e. multiple food spots). The results of the strain-specific simulations were

confirmed by experiments that demonstrate faster food depletion by N2 than by *npr-1* worms regardless of food spot numbers. Assuming fast food depletion as a fitness advantage, these results agree with a previous study reporting that the aggregating strains are less fit in laboratory conditions (41). Another recent study shows that the observed fitness advantage of N2 over *npr-1* worms is in fact dissociable from their aggregation phenotypes (30). Indeed, we conducted further simulations using a modified strain-specific model to show that N2's better foraging performance may be more attributable to other behavioural differences such as higher feeding rate, than to its solitary foraging strategy. Therefore our strain-specific model suggests that collective foraging is not an efficient strategy, at least under our tested food distribution conditions, while our minimal model indicates that this remains a theoretical possibility.

The question remains why *C. elegans* wild strains aggregate into groups, if it is not essential for foraging success in a patchy food distribution environment? One possible explanation is that the patchy food distribution environment (with multiple food spots) that we computationally and experimentally created here does not represent the actual ecological context of *C. elegans*, which we know surprisingly little about (24, 42). The food clusters in the real natural environment may well be several orders of magnitude further apart from each other than what we tested with the multiple food spot experiments here, and with temporal fluctuations and varying quality which we have not considered here. Therefore our simulation and experimental results regarding foraging success in patchy food distributions may not be so "patchy" or "realistic" in the end to conclude that wild *C. elegans* do not benefit from collective foraging in their natural resource environments. Regardless of food distribution, aggregation may nevertheless serve as a mechanism for protecting *C. elegans* from dangers associated with the high-oxygen surface environment (such as desiccation or UV radiation) (43) or from pathogens that infect the worm through its cuticle (36), so collective foraging

may be a means to balance the costs of foraging with the benefits of avoiding such dangers. Moreover, our simulation results provide yet another hypothesis: while collective foraging may decrease the overall foraging efficiency of the social strain, it could also reduce the number of worms at the risk of extreme starvation (Figure S5). This view is consistent with optimal foraging theory which typically considers optimal movement strategies and the trade-off between exploitation and exploration (34, 44-47). Joining groups may enhance foraging in environments with big food clusters and decrease the variance of foraging success (47), which is recapitulated by our minimal and strain-specific models, respectively.

In conclusion, our simulations and experiments were designed to test whether collective foraging helps to consume patchily distributed food, which may be representative of resource distributions in the wild. While we conclude that it does in our minimal model, in the more realistic simulations incorporating strain-specific behavioural parameters, the solitary agents deplete food faster and have a higher median efficiency of food uptake, and so outperform the social agents at a population level. However, social agents are better at preventing starvation of its individuals. Our simulations only considered spatial variation in the food distributions, but have not explored temporal fluctuations of the environment. The dynamics of environmental fluctuations have been shown to influence whether sensing or stochastic phenotype switching is favoured in growing populations (48). An alternative approach is to consider under what environmental conditions collective foraging strategies emerge by evolution (49). Thus the role of both fluctuating environments and evolution of foraging strategies are avenues for further work on the benefits of collective foraging strategies.

Material and Methods

Basic simulation rules

The following basic rules apply to all simulations: Parameter n represents the number of agents ($n = 40$) simulated on a square-lattice with L^2 lattice sites ($L = 35$) using periodic boundary conditions (15). The direct neighbourhood of an agent is defined as the eight surrounding lattice sites, whereas the 16 lattice sites surrounding the direct neighbourhood are defined as the remote neighbourhood (Figure 2a). Each lattice site contains a certain number of food units depending on the underlying food distribution. Volume exclusion is enforced in all simulations so that every lattice site can only be occupied by a single agent. We use random initial positions of the agents. At every time step, each agent checks if there is food at its current position, eats one food unit (if there are any) and then attempts to move. All simulations are implemented with MATLAB R2017a. Simulations are run 500 times for each condition, using the same initial distribution of food and agents. For every simulation the time taken to 90% food depletion is measured for the population, and the foraging efficiency and the total food uptake are measured for individual agents.

Food distribution in simulations

Two different types of food distributions are used in the simulations. The first type is used for the minimal simulations, where food distribution is parameterised by γ ($\gamma = 0, 1, 1.5, 2, 3$), which controls the degree of clustering (Figure 3a) (15). For $\gamma > 0$, every new food unit is placed at a distance d ($1 \leq d \leq \frac{L}{\sqrt{2}}$) in a random direction to a random existing food unit. For $\gamma = 0$ the food is distributed uniformly random on the lattice. For $\gamma > 0$ the distance d is calculated as follows: $d = r^{\frac{-1}{\gamma}}$, where r is a random number distributed uniformly between 0 and 1. If d is larger than $L/\sqrt{2}$, a uniform random value between 1 and $L/\sqrt{2}$ is chosen

instead. The value of d is calculated independently for every food unit. To initialise simulations, one food unit is placed on a randomly chosen lattice site and then the remaining food units are distributed accordingly. For strain-specific simulations we use the second type of food distribution, where one, two, or four food spots are distributed on the lattice and food is distributed evenly within the spot (Figure 4a). The total food level is the same among simulations for the minimal model ($L^2 \cdot 10$), but slightly varies for the strain-specific model depending on the number of food spots (because each spot has to be made up of an integer number of lattice sites). To ensure consistent comparisons, we calculated the time to consuming $L^2 \cdot 10 \cdot 0.9$ food units as time to depletion for every simulation.

Minimal model simulations

Minimal model simulations are conducted with parameters listed in Table 2. The basics of random and targeted steps are explained in the main text (Figure 2), and a flow chart is provided in Figure S1a. Food is perceived on the lattice site the agent occupies and in the direct neighbourhood. Agents try all possible lattice sites until it finds an available site unoccupied by another agent. If no such site is available, the agent remains in its current position. Social agents perform a targeted step when food is present and at least one other agent is present in its direct neighbourhood. In this case, the agent moves randomly to one of the lattice sites located next to another agent in the direct neighbourhood (Figure 2b,c). For the calculation of individual efficiencies, moving to the remote neighbourhood counts as two steps, moving to the direct neighbourhood counts as one step, and if the agent remains at its position then it counts as zero step.

Strain-specific model simulations

The parameters for strain-specific simulations are given in Table 2, and a flow chart is provided in Figure S1b. In these simulations, agents sense food only on the lattice site they

occupy. The strain-specific model incorporates food-leaving probability ρ (see Supplementary Methods), which is set to zero for our simulation results here. Foraging efficiencies for strain-specific simulations are calculated in a manner similar to that for the minimal model simulations.

Experimental procedure to validate the strain-specific simulations

The experimental procedures used here are identical to the "Bright field standard swarming imaging" method that we previously published (26). A step-by-step protocol is available at http://dx.doi.org/10.17504/protocols.io.vyhe7t6. Briefly, 35 mm imaging plates containing low peptone NGM agar are freshly seeded with 20 µL of diluted *E. coli* OP50 bacteria (OD_{600} = 0.75) shortly before imaging, with the 20 µL equally divided between the required number of food spots to produce different patchiness conditions (i.e., four spots of 5 µL each, two spots of 10 µL each, or one spot with 20 µL). Forty age-synchronised young adult worms are washed and transferred onto the imaging plate in a liquid drop without disturbing the bacterial spots, and imaging commences immediately. Time-lapse images were recorded at 25 fps for 7 hours at 20° C with Gecko software (v2.0.3.1) and a custom-built six-camera rig equipped with Dalsa Genie cameras (G2-GM10-T2041). The images were segmented in real time and automated animal tracking was conducted with the Tierpsy Tracker software (v1.3) (50) to extract speed. Three to four replicates of the experiments are available for each combination of worm strain and food distribution condition.

Estimating the time to food depletion from experimental data

As worms speed up when food becomes depleted, we identified increases in the mean worm speed as a proxy for food depletion. The recordings were first analysed by eye to find periods of increased activity which helped to identify the corresponding peak in speed. As imaging commenced as soon as worms were transferred to the imaging plate in a liquid drop, the

foraging start time is manually defined as the moment when the liquid drop completely absorbs into the media allowing all worms to crawl out. To identify periods with increased speed, we followed mean worm speed (calculated per second) over the duration of the recordings. Mean speed is smoothed with a window size of 500 seconds centred on the current time to give distinguishable peaks in speed. Note that plots can have more than one local maximum for experiments with more than one food spot, as the food spots are not depleted simultaneously. In this case, the last local maximum is defined as the time in which most bacteria are depleted (Figure S6a-c).

Acknowledgements

We would like to thank Camille Straboni from the Brown lab for providing additional brightfield movies. Some strains were provided by the CGC, which is funded by NIH Office of Research Infrastructure Programs (P40 OD010440).

Funding

This work was funded by the Biotechnology and Biological Sciences Research Council through grant BB/N00065X/1 to AEXB and RGE, and by the Medical Research Council through grant MC-A658-5TY30 to AEXB.

References

1. Partridge BL. The structure and function of fish schools. Sci Am. 1982;246(6):114-23.
2. Emlen JT, Jr. Flocking behavior in birds. The Auk. 1952;69:160-70.
3. Gager Y, Gimenez O, O'Mara MT, Dechmann DK. Group size, survival and surprisingly short lifespan in socially foraging bats. BMC Ecol. 2016;16:2.
4. Foster WA, Treherne JE. Evidence for the Dilution Effect in the Selfish Herd from Fish Predation on a Marine Insect. Nature. 1981;293(5832):466-7.

5. Krause J, Ruxton GD, Krause S. Swarm intelligence in animals and humans. Trends Ecol Evol. 2010;25(1):28-34.

6. Ward AJ, Herbert-Read JE, Sumpter DJ, Krause J. Fast and accurate decisions through collective vigilance in fish shoals. Proceedings of the National Academy of Sciences of the United States of America. 2011;108(6):2312-5.

7. Cafazzo S, Bonanni R, Valsecchi P, Natoli E. Social Variables Affecting Mate Preferences, Copulation and Reproductive Outcome in a Pack of Free-Ranging Dogs. Plos One. 2014;9(6).

8. Markham AC, Gesquiere LR. Costs and benefits of group living in primates: an energetic perspective. Philos Trans R Soc Lond B Biol Sci. 2017;372(1727).

9. Wittwer B, Hefetz A, Simon T, Murphy LEK, Elgar MA, Pierce NE, et al. Solitary bees reduce investment in communication compared with their social relatives. Proceedings of the National Academy of Sciences of the United States of America. 2017;114(25):6569-74.

10. Dechaume-Moncharmont FX, Dornhaus A, Houston AI, McNamara JM, Collins EJ, Franks NR. The hidden cost of information in collective foraging. Proc Biol Sci. 2005;272(1573):1689-95.

11. Snijders L, Kurvers RHJM, Krause S, Ramnarine IW, Krause J. Individual- and population-level drivers of consistent foraging success across environments. bioRxiv. 2018.

12. Li L, Peng H, Kurths J, Yang Y, Schellnhuber HJ. Chaos-order transition in foraging behavior of ants. Proceedings of the National Academy of Sciences of the United States of America. 2014;111(23):8392-7.

13. Torney CJ, Berdahl A, Couzin ID. Signalling and the Evolution of Cooperative Foraging in Dynamic Environments. Plos Computational Biology. 2011;7(9).

14. Cvikel N, Berg KE, Levin E, Hurme E, Borissov I, Boonman A, et al. Bats Aggregate to Improve Prey Search but Might Be Impaired when Their Density Becomes Too High. Current Biology. 2015;25(2):206-11.

15. Bhattacharya K, Vicsek T. Collective foraging in heterogeneous landscapes. Journal of the Royal Society Interface. 2014;11(100).

16. Beauchamp G. Exploring the role of vision in social foraging: what happens to group size, vigilance, spacing, aggression and habitat use in birds and mammals that forage at night? Biol Rev Camb Philos Soc. 2007;82(3):511-25.

17. Berdahl AM, Kao AB, Flack A, Westley PAH, Codling EA, Couzin ID, et al. Collective animal navigation and migratory culture: from theoretical models to empirical

evidence. Philosophical Transactions of the Royal Society B-Biological Sciences. 2018;373(1746).

18. Corsi AK, Wightman B, Chalfie M. A Transparent Window into Biology: A Primer on Caenorhabditis elegans. Genetics. 2015;200(2):387-407.

19. Brenner S. The genetics of Caenorhabditis elegans. Genetics. 1974;77(1):71-94.

20. Boulin T, Hobert O. From genes to function: the C. elegans genetic toolbox. Wiley Interdiscip Rev Dev Biol. 2012;1(1):114-37.

21. Consortium CeS. Genome sequence of the nematode C. elegans: a platform for investigating biology. Science. 1998;282(5396):2012-8.

22. Cook SJ, Jarrell TA, Brittin CA, Wang Y, Bloniarz AE, Yakovlev MA, et al. Whole-animal connectomes of both Caenorhabditis elegans sexes. Nature. 2019;571(7763):63-71.

23. Felix MA, Braendle C. The natural history of Caenorhabditis elegans. Curr Biol. 2010;20(22):R965-9.

24. Frezal L, Felix MA. C. elegans outside the Petri dish. eLife. 2015;4.

25. de Bono M, Bargmann CI. Natural variation in a neuropeptide Y receptor homolog modifies social behavior and food response in C. elegans. Cell. 1998;94(5):679-89.

26. Ding SS, Schumacher LJ, Javer AE, Endres RG, Brown AE. Shared behavioral mechanisms underlie C. elegans aggregation and swarming. eLife. 2019;8.

27. Gray JM, Karow DS, Lu H, Chang AJ, Chang JS, Ellis RE, et al. Oxygen sensation and social feeding mediated by a C. elegans guanylate cyclase homologue. Nature. 2004;430(6997):317-22.

28. Macosko EZ, Pokala N, Feinberg EH, Chalasani SH, Butcher RA, Clardy J, et al. A hub-and-spoke circuit drives pheromone attraction and social behaviour in C. elegans. Nature. 2009;458(7242):1171-5.

29. Reddy KC, Andersen EC, Kruglyak L, Kim DH. A polymorphism in npr-1 is a behavioral determinant of pathogen susceptibility in C. elegans. Science. 2009;323(5912):382-4.

30. Zhao Y, Long L, Xu W, Campbell RF, Large EE, Greene JS, et al. Changes to social feeding behaviors are not sufficient for fitness gains of the Caenorhabditis elegans N2 reference strain. eLife. 2018;7.

31. Gray JM, Hill JJ, Bargmann CI. A circuit for navigation in Caenorhabditis elegans. Proceedings of the National Academy of Sciences of the United States of America. 2005;102(9):3184-91.

32. Scholz M, Dinner AR, Levine E, Biron D. Stochastic feeding dynamics arise from the need for information and energy. Proceedings of the National Academy of Sciences of the United States of America. 2017;114(35):9261-6.

33. Riddle DL, Blumenthal T, Meyer BJ, Priess JR. Introduction to C. elegans. In: nd, Riddle DL, Blumenthal T, Meyer BJ, Priess JR, editors. C elegans II. Cold Spring Harbor (NY)1997.

34. Charnov EL. Optimal foraging, the marginal value theorem. Theor Popul Biol. 1976;9(2):129-36.

35. Wajnberg E, Fauvergue X, Pons O. Patch leaving decision rules and the Marginal Value Theorem: an experimental analysis and a simulation model. Behavioral Ecology. 2000;11(6):577-86.

36. Ding SS, Sarkisyan KS, Brown AEX. Measuring C. elegans spatial foraging and food intake using bioluminescent bacteria. bioRxiv. 2019.

37. Milward K, Busch KE, Murphy RJ, de Bono M, Olofsson B. Neuronal and molecular substrates for optimal foraging in Caenorhabditis elegans. Proceedings of the National Academy of Sciences of the United States of America. 2011;108(51):20672-7.

38. Shtonda BB, Avery L. Dietary choice behavior in Caenorhabditis elegans. J Exp Biol. 2006;209(Pt 1):89-102.

39. Abel JH, Drawert B, Hellander A, Petzold LR. GillesPy: A Python Package for Stochastic Model Building and Simulation. IEEE Life Sci Lett. 2016;2(3):35-8.

40. Hein AM, Rosenthal SB, Hagstrom GI, Berdahl A, Torney CJ, Couzin ID. The evolution of distributed sensing and collective computation in animal populations. eLife. 2015;4:e10955.

41. Andersen EC, Bloom JS, Gerke JP, Kruglyak L. A variant in the neuropeptide receptor npr-1 is a major determinant of Caenorhabditis elegans growth and physiology. PLoS Genet. 2014;10(2):e1004156.

42. Felix MA, Duveau F. Population dynamics and habitat sharing of natural populations of Caenorhabditis elegans and C. briggsae. BMC Biol. 2012;10:59.

43. Busch KE, Olofsson B. Should I stay or should I go? Worm. 2012;1(3):182-6.

44. Calhoun AJ, Chalasani SH, Sharpee TO. Maximally informative foraging by Caenorhabditis elegans. eLife. 2014;3.

45. Chupeau M, Benichou O, Redner S. Search in patchy media: Exploitation-exploration tradeoff. Phys Rev E. 2017;95(1-1):012157.

46. Volpe G, Volpe G. The topography of the environment alters the optimal search strategy for active particles. Proceedings of the National Academy of Sciences of the United States of America. 2017;114(43):11350-5.

47. Giraldeau LA, Beauchamp G. Food exploitation: searching for the optimal joining policy. Trends Ecol Evol. 1999;14(3):102-6.

48. Kussell E, Leibler S. Phenotypic diversity, population growth, and information in fluctuating environments. Science. 2005;309(5743):2075-8.

49. Witkowski O, Ikegami T. Emergence of Swarming Behavior: Foraging Agents Evolve Collective Motion Based on Signaling. Plos One. 2016;11(4).

50. Javer A, Currie M, Lee CW, Hokanson J, Li K, Martineau CN, et al. An open-source platform for analyzing and sharing worm-behavior data. Nat Methods. 2018;15(9):645-6.

Supplementary Material

Supplementary Material accompanies this publication.

Data accessibility

The codes for the models and for data analysis can be found at

https://github.com/lsmuhle/CollectiveFeeding.

Competing interests

We have no competing interests.

Author contributions

SSD performed the experiments. SSD and LSM conducted the analysis of experimental data. LSM, LJS and RGE designed the models. LSM implemented the models and conducted the analysis of the simulations with supervision and assistance from LJS and RGE. The manuscript was written and revised by all authors.